Modeling the Low Velocity Impact on Thick-Section Composite Cylinder

Sang-Guk Kang[1], Bazle A. Gama[1, ♦], Shridhar Yarlagadda,
John W. Gillespie Jr.[1,2,3], Thorsten Schütz[4], and Stephan Fell[4]

[1] *University of Delaware - Center for Composite Materials (UD-CCM)*
[2] *Department of Materials Science and Engineering*
[3] *Department of Civil and Environmental Engineering*
University of Delaware, Newark, DE 19716
[4] *Adam Opel GmbH, GM Alternative Propulsion Center Europe*
IPC MK-01, D-65423 Rüsselsheim (Germany).

Abstract

Composite materials frequently have been applied to axi-symmetric filament-wound cylinder structures due to their specific stiffness and strength properties. When these structures are subjected to low-velocity impact (LVI), there exists a possibility of significant material damage which can drastically reduce the structural performance. The main objective of this paper is to predict the low velocity impact damage in thick composite cylinders using MAT162 progressive damage model implemented in LS-DYNA®. In this paper, damage prediction of a thick composite cylinder under low-velocity impact using uni-directional (UD) composite model of MAT162 is presented. A finite element model (FEM) of a thick composite cylinder with appropriate boundary conditions is developed to predict impact damages under different impact energies of a cylindrical steel impactor. Dynamic deformation, damage progression, and energy dissipation of the composite cylinder under LVI loading as a function of impact energy are presented.

Introduction

Filament winding is a popular fabrication technique for axi-symmetric composite structures for pressure vessel applications. Understanding the performance and mechanical behavior of composite pressure vessels under low velocity impact (LVI) scenarios is necessary to confidently deploy such structures to field applications. Generally, LVI is known to cause critical structural safety problems such as matrix crack and delamination although it is a non-penetrating impact for which stress wave propagation through the thickness plays no significant role. [1].

In this paper, damage prediction of a thick composite cylinder under LVI is presented using the state-of-the-art progressive composite damage model, MAT162 in LS-DYNA. MAT162 has the capability of modeling both damage initiation and propagation. In addition, it is able to model both uni-directional (UD) and plain-weave (PW) material behavior, which is an advantage since UD tows are used for filament winding. A finite element model of a thick composite cylinder with appropriate boundary conditions is developed to predict the impact damages under different impact energies for a cylindrical steel impactor. Modeling issues, dynamic deformation, damage

♦ Corresponding Author, Tel: (302) 831-0248, E-mail: gama@udel.edu

progression, and energy dissipation of the composite cylinder under LVI loading as a function of impact energy are presented.

MAT162 Implemented in LS-DYNA

MAT162, implemented in LS-DYNA, is a progressive composite damage model developed by Material Sciences Corporation (MSC) and University of Delaware Center for Composite Materials (UD-CCM). MAT162 has the capability of modeling the onset and progression of damage for both uni-directional (UD) and plain weave (PW) composites. It is based on Hashin's quadratic failure criteria [2] and Matzenmiller's progressive damage model with softening parameters [3]. Applications of MAT162 PW composite module can be found in Ref. [4-6], however, applications of MAT162 UD composite module can hardly be found. In addition to progressive composite damage, MAT162 can include strain rate effects on modulus and strengths in terms of strain rate parameters [7].

Failure criteria for UD and PW composites are summarized in Table 1. As shown in Table 1, MAT162 can simulate various damage modes including fiber damage (tension/shear, compression, and crush) and matrix damage such as matrix cracking and delamination by the use of four softening parameters (m1, m2, m3, and m4). m1 and m2 control the tensile/compressive softening of reinforcing fibers along X and Y direction (Fill and Warp directions), respectively. m3 controls softening of crush and punch shear of fiber, and m4 is related to all the matrix damage such as matrix cracking and delamination. Damage function φ describes the fraction of stiffness degradation and is defined for each damage mode as expressed in Eq. (1).

$$\varphi = 1 - e^{\frac{1}{m}(1-r^m)} \tag{1}$$

where *m* is a softening parameter of a material, and *r* is the damage threshold which has the initial value of unity before the damage initiates, and are updated due to damage accumulation in the associated damage modes. Since different failure modes (φ_j) affect a specific material degradation, MAT 162 defines the maximum damage variable as the modulus reduction parameter (ω_i):

$$\omega_i = \max\{\varphi_j q_{ij}\} \qquad i = 1,2,...,6, \quad \begin{matrix} j = 1,2,...,6 \ \textbf{(UD)} \\ j = 1,2,...,7 \ \textbf{(PW)} \end{matrix} \tag{2}$$

where q_{ij} relates the individual damage variables φ_j to the various damage modes provided by the damage functions of the UD and PW fabric models.

$$[q_{uni}] = \begin{bmatrix} 1 & 1 & 1 & 0 & 0 & 0 \\ 0 & 0 & 1 & 1 & 1 & 0 \\ 0 & 0 & 1 & 0 & 0 & 1 \\ 1 & 1 & 1 & 1 & 1 & 0 \\ 0 & 0 & 1 & 1 & 1 & 1 \\ 1 & 1 & 1 & 0 & 0 & 1 \end{bmatrix}, \quad [q_{fabric}] = \begin{bmatrix} 1 & 0 & 1 & 0 & 1 & 0 & 0 \\ 0 & 1 & 0 & 1 & 1 & 0 & 0 \\ 0 & 0 & 0 & 0 & 1 & 0 & 1 \\ 1 & 1 & 1 & 1 & 1 & 1 & 0 \\ 0 & 1 & 0 & 1 & 1 & 0 & 1 \\ 1 & 0 & 1 & 0 & 1 & 0 & 1 \end{bmatrix} \tag{3}$$

Table 1. Failure criterion of MAT162 progressive damage model

Uni-Directional Composite		**Plain-Weave Composite**	
Damage Mode	**Criterion**	**Damage Mode**	**Criterion**
Fiber tension/shear	$\left(\frac{E_1.\langle \varepsilon_1 \rangle}{X_{1,T}}\right)^2 + \frac{G_{12}^2 \varepsilon_{12}^2 + G_{31}^2 \varepsilon_{31}^2}{S_{FS}^2} = r_1^2$	Fill Fiber tension/shear	$\left(\frac{E_1.\langle \varepsilon_1 \rangle}{X_{1,T}}\right)^2 + \left(\frac{G_{31}\varepsilon_{31}}{S_{FS}}\right)^2 = r_1^2$
Fiber compression	$\left(\frac{E_1.\langle \varepsilon_1' \rangle}{X_{1,C}}\right)^2 = r_2^2$, $\varepsilon_1' = -\varepsilon_1 - \frac{\langle -E_2\varepsilon_2 - E_3\varepsilon_3 \rangle}{2E_1}$	Fill Fiber compression	$\left(\frac{E_1.\langle \varepsilon_1' \rangle}{X_{1,C}}\right)^2 = r_2^2 \quad \varepsilon_1' = -\varepsilon_1 - \langle -\varepsilon_3 \rangle \frac{E_3}{E_1}$
Fiber crush	$\left(\frac{E_3 \langle -\varepsilon_3 \rangle}{S_{FC}}\right)^2 = r_3^2$	Warp Fiber tension/shear	$\left(\frac{E_2.\langle \varepsilon_2 \rangle}{X_{2,T}}\right)^2 + \left(\frac{G_{23}\varepsilon_{23}}{S_{FS}}\right)^2 = r_3^2$
Transverse compression	$\left(\frac{E_2 \langle -\varepsilon_2 \rangle}{X_{2,C}}\right)^2 = r_4^2$	Warp Fiber compression	$\left(\frac{E_2.\langle \varepsilon_2' \rangle}{X_{2,C}}\right)^2 = r_4^2$, $\varepsilon_2' = -\varepsilon_2 - \langle -\varepsilon_3 \rangle \frac{E_3}{E_2}$
Perpendicular matrix crack	$\left(\frac{E_2.\langle \varepsilon_2 \rangle}{X_{2,T}}\right)^2 + \left(\frac{G_{23}.\varepsilon_{23}}{S_{23}+S_{SRB}}\right)^2 + \left(\frac{G_{12}.\varepsilon_{12}}{S_{12}+S_{SRB}}\right)^2 = r_5^2$	Fiber crush	$\left(\frac{E_3 < -\varepsilon_3 >}{S_{FC}}\right)^2 = r_5^2$
Parallel matrix (Delamination)	$S^2 \left\{ \left(\frac{E_3.\langle \varepsilon_3 \rangle}{X_{3,T}}\right)^2 + \left(\frac{G_{23}.\varepsilon_{23}}{S_{23}+S_{SRC}}\right)^2 + \left(\frac{G_{31}.\varepsilon_{31}}{S_{31}+S_{SRC}}\right)^2 \right\} = r_6^2$	Perpendicular matrix crack	$\left(\frac{G_{12}\varepsilon_{12}}{S_{12}}\right)^2 = r_6^2$
* $S_{SRB} = E_2 \tan(\phi) \langle -\varepsilon_2 \rangle$ $S_{SRC} = E_3 \tan(\phi) \langle -\varepsilon_3 \rangle$		Parallel matrix (Delamination)	$S^2 \left\{ \left(\frac{E_3.\langle \varepsilon_3 \rangle}{S_{3,T}}\right)^2 + \left(\frac{G_{23}.\varepsilon_{23}}{S_{23}+S_{SRC}}\right)^2 + \left(\frac{G_{31}.\varepsilon_{31}}{S_{31}+S_{SRC}}\right)^2 \right\} = r_7^2$

Using Eq. (2), a new compliance matrix ($[\mathbf{S}]$) is obtained to model progressive damage as expressed in Eq. (4).

$$[\mathbf{S}] = \begin{bmatrix} \frac{1}{(1-\omega_1)E_1} & \frac{-\nu_{21}}{E_2} & \frac{-\nu_{31}}{E_3} & 0 & 0 & 0 \\ \frac{-\nu_{12}}{E_1} & \frac{1}{(1-\omega_2)E_2} & \frac{-\nu_{32}}{E_3} & 0 & 0 & 0 \\ \frac{-\nu_{13}}{E_1} & \frac{-\nu_{23}}{E_2} & \frac{1}{(1-\omega_3)E_3} & 0 & 0 & 0 \\ 0 & 0 & 0 & \frac{1}{(1-\omega_4)G_{12}} & 0 & 0 \\ 0 & 0 & 0 & 0 & \frac{1}{(1-\omega_5)G_{23}} & 0 \\ 0 & 0 & 0 & 0 & 0 & \frac{1}{(1-\omega_6)G_{31}} \end{bmatrix} \tag{4}$$

Finite Element Model of the Composite Cylinder

The composite cylinder has 24 layers composed of 11 hoop and 13 helical layers. It is made by carbon fiber reinforced plastic (CFRP), and its material properties for MAT162 model input were measured through ASTM standardized tests and non-standardized tests such as punch shear tests. The cylinder is 300 mm in length and has an inner diameter of 238 mm. Each layer is 0.8 mm in thickness, and total thickness of the cylinder is 19.2 mm. In order to get reasonable computational cost and time as well as accurate results, a sufficient but not excessive number of elements is necessary. Because the cylinder is modeled layer by layer to predict the delamination, 37 parts (11 hoop + 2×13 helical, 1 part per hoop layer and 2 parts per helical layer) for the cylinder modeling are generated. In addition, 3 elements through thickness are used for a hoop layer and 2 elements for the helical layers. This is because more elements through thickness direction give more precise predictions of delamination. Thus, 85 elements are used in the through-thickness direction (11×3 + 13×2×2) of the cylinder. A cylinder shell was modeled as shown in Fig. 1, from which full solid elements are generated through radial extrusion. Total number of elements of the cylinder shell is 9,628. In addition, mesh is effectively distributed all over the cylinder surface considering impact location. The elements near the impactor and fixture areas are refined, and the mesh density becomes reduced toward the outside of these regions.

In order to reduce the contact conditions to a minimum, we have divided the cylinder shell into 7 different parts as shown in Fig. 1 (6 parts is shown in Fig. 1, and 1 part is hidden in the back). The X axis is aligned with the axis of the cylinder, and Z axis with the direction of the impactor motion. According to this axis orientation, Fig. 1 shows the X-Y plane view of the cylinder. The number of elements of the full cylinder model is 835,060. Figs. 2 and 3 show a side view and a cross-sectional view of the composite FE model, respectively. The number of elements used through the thickness direction is shown from Fig. 3.

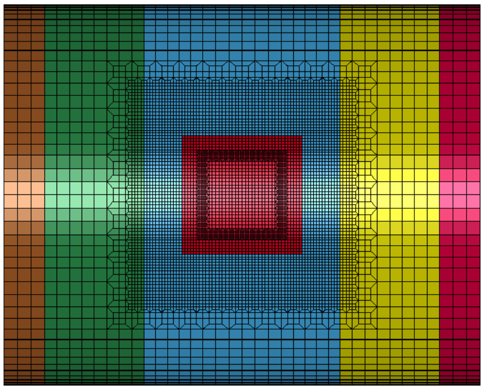

Fig. 1. Cylinder shell to expand into cylinder solid elements

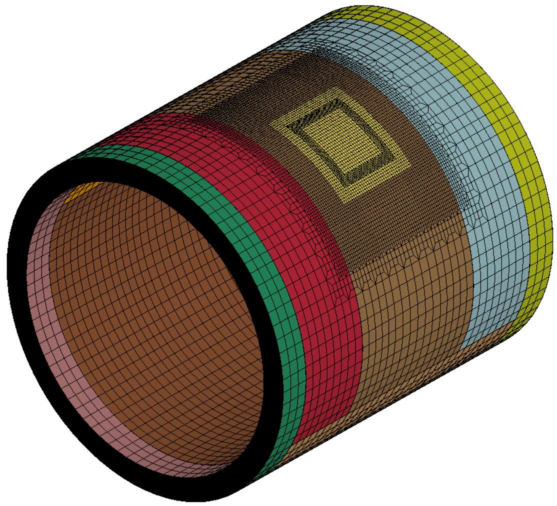

Fig. 2. Final FE model of the composite cylinder

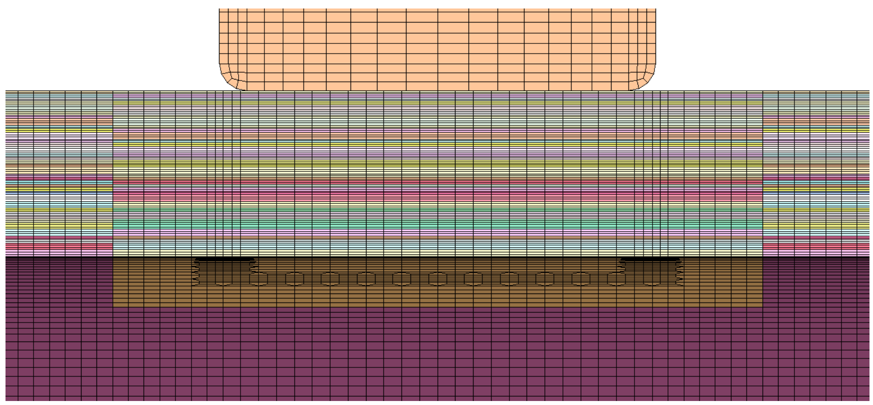

Fig. 3. Cross-section of the composite cylinder with the impactor

FE Models for the Impactor and the Fixture

A circular steel impactor of 50 mm diameter is used in this simulation. A set of point masses were applied to the nodes on the top surface of the impactor as shown in Fig. 4, such that the total mass will be the same as that of the full impacting structure, which is 350 kg. Fig. 5 shows the FE model of two solid steel fixtures for the LVI experiments. Sharp edges were rounded in order to prevent any penetration of nodes. Fig. 6 shows the final assembly of each part for LVI test fixture with the thick section composite cylinder, and detailed information on this model is given in Table 2. Total number of elements of the full model is calculated to be 849,740.

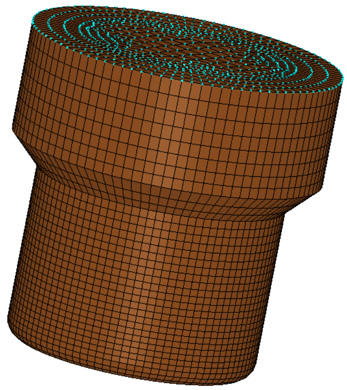

Fig. 4. Impactor with point masses

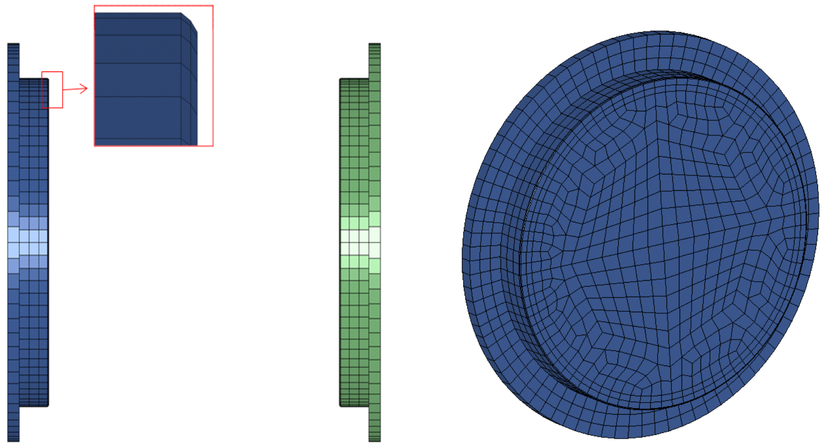

Fig. 5. FE model of solid steel fixture, and its mesh distribution

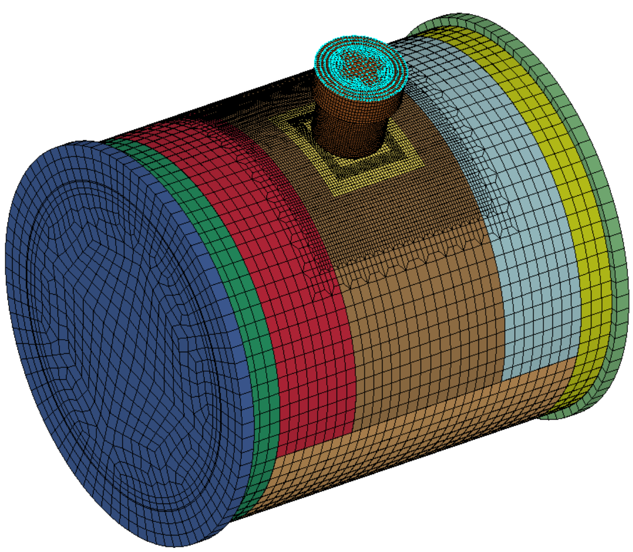

Fig. 6. Final FE Model of LVI on thick section composite cylinder

Table 2. Information on FE Model for LVI simulation

Part	# of Elements (Total: 849,740)	Remarks
Cylinder	818,380	Hoop: 3 elms/layer Helical: +θ(2elms)/-θ(2elms) # of parts in a layer: 7 # of total parts: 259
Fixture	6,832	# of total parts: 2
Impactor	24,528	Total weight: 350kg

Loading, Boundary, and Contact Conditions

Various energy levels were investigated. Since the weight of the impactor is fixed, it is necessary to calculate the required velocities in order to get the desired energy levels.
Kinetic energy of the impactor is expressed as:

$$E = \frac{1}{2} m v^2 \tag{5}$$

Then, the corresponding impact velocity can be written as:

$$v = \sqrt{\frac{2E}{m}} \tag{6}$$

In order to prevent the solid fixtures from moving during impact, both outer ends of the fixtures were given clamped conditions, i.e., no displacement and no rotation along x, y and z axis. The LS-DYNA keyword, CONTACT_ERODING_SINGLE_SURFACE is used to define contact between the impactor and the closest composite cylinder parts. The contact definition is defined between the fixture and the composite cylinder using CONTACT_AUTOMATIC_SURFACE_TO_SURFACE.

Results and Discussion

Numerical impact on the cylinder is performed at several energy levels. The highest impact energy (E_{max}) which shows the maximum load (P_{max}) that the cylinder can withstand is chosen as the baseline impact case. The maximum impact energy (E_{max}), the maximum load (P_{max}), the time (t_{max}) and displacement (d_{max}) at maximum load are used to make the impact responses dimensionless. Figs. 7 and 8 show the normalized contact force between the composite cylinder and the impactor as a function of normalized time and normalized displacement, respectively.
With the increase in impact energy, the peak force and duration of contact increase, while the locus of force-displacement in the loading section does not change with impact energy. It is the unloading part of the force displacement which is different for different impact energies. This is

a typical phenomenon reported in literature [8, 9], and is presented in Figure 9. The area bounded by the loading and unloading curves represents the energy dissipation during an impact event. Comparing the present numerical prediction with literature reveals that the energy-dissipating damage mechanisms can be captured in numerical space. In addition, the evolution of impact damage as a function of time can be visualized from numerical simulation (Fig. 10). Fig. 10 shows an example of delamination propagation of the composite cylinder at a certain energy level ($E/E_{max} = 0.220$). For this energy level, the velocity of the projectile becomes zero at $t/t_{max} = 1.227$. It can be shown that significant delamination damages inside the thick composite cylinder are induced near the impactor and fixture edges by low velocity impact, and they continuously propagated throughout the cylinder while the impactor bounced back.

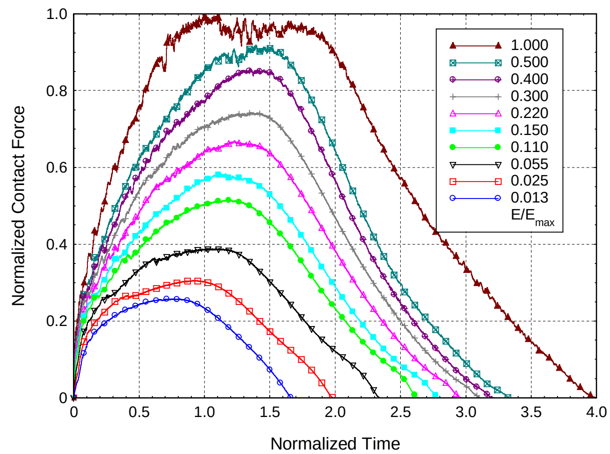

Fig. 7. Normalized contact force vs. normalized time curve

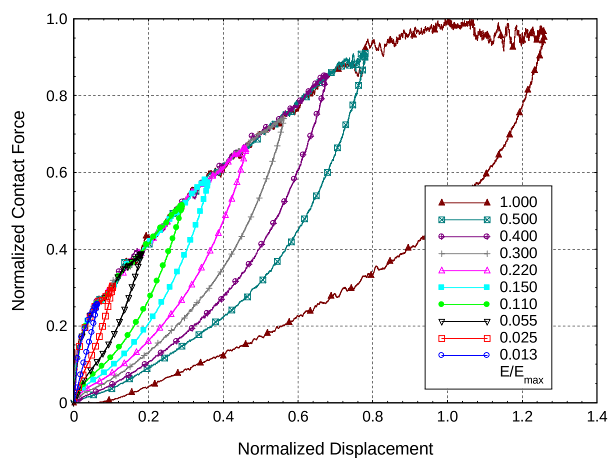

Fig. 8. Normalized contact force vs. normalized displacement curve

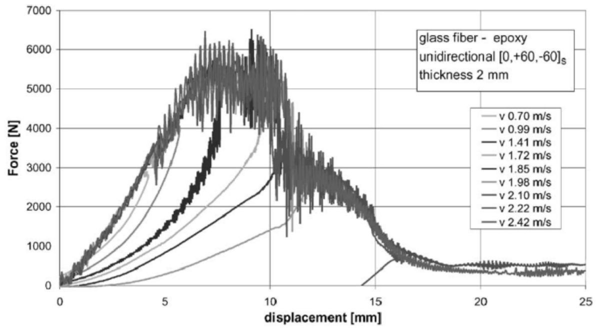

(a) Ref. [8], Belingardi and Vadori (2002)

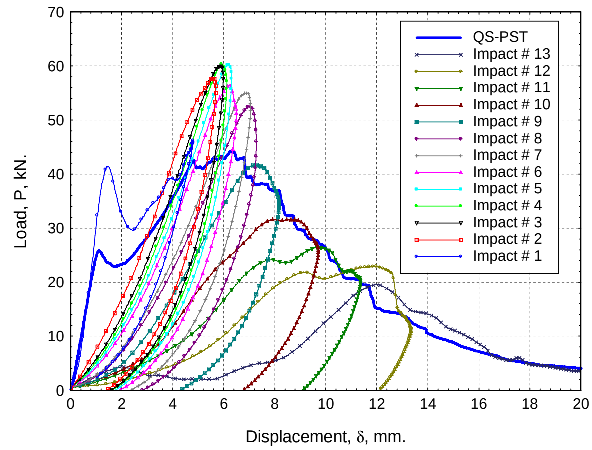

(b) Ref. [9], Gama et al. (2005)

Fig. 9. Low velocity impact response as a function of impact energy from literature

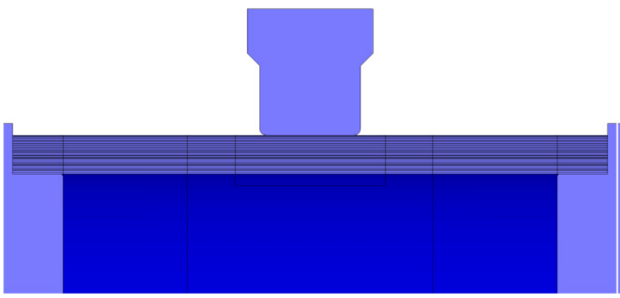

(a) $t/t_{max} = 0$

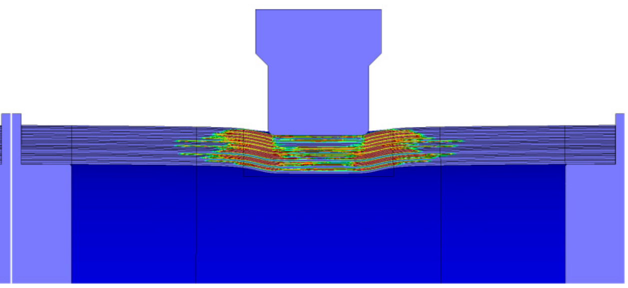

(b) $t/t_{max} = 0.153$

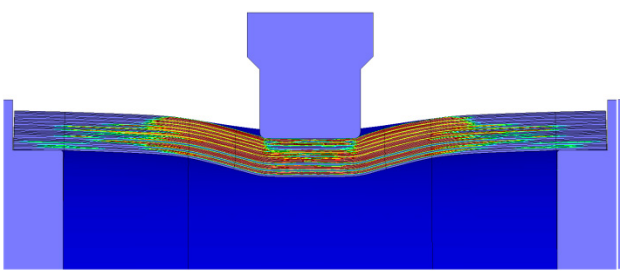

(c) $t/t_{max} = 0.460$

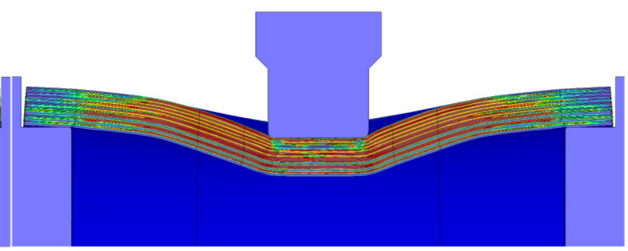

(d) $t/t_{max} = 1.227$ ($V_{impactor} = 0$)

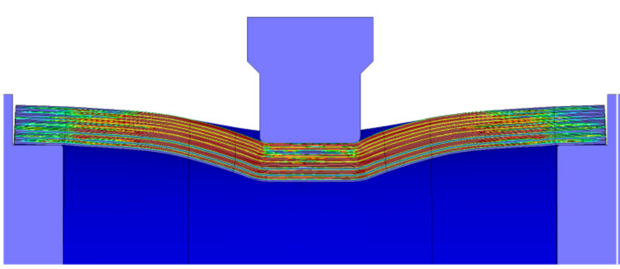

(e) $t/t_{max} = 1.994$

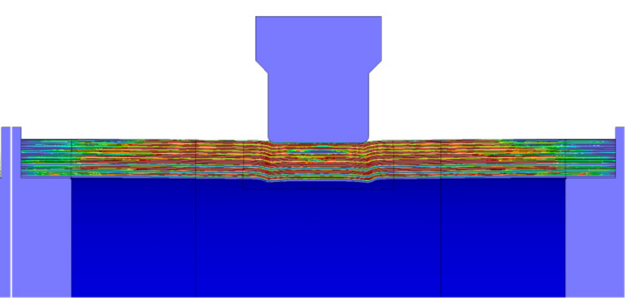

(f) $t/t_{max} = 2.761$

Fig. 10. Propagation of delaminations inside the composite cylinder ($E/E_{max} = 0.220$)

Summary

A series of finite element simulations of low velocity impact on a thick section composite cylinder is presented using the state-of-the-art progressive composite damage model, MAT162. Modeling issues such as the filament wound composite cylinder with multiple unidirectional hoop and helical layers, the impactor and the solid fixtures were discussed in detail. For this finite element model, various impact energies were applied with different impact velocities, and the results including deformation, damage progression, and energy dissipation of the composite cylinder as a function of impact energy were discussed. It has been shown that MAT162 can be effectively used to simulate the progressive damage of filament wound thick section composite cylinders under low velocity impact loading.

Acknowledgement

The authors gratefully acknowledge the funding provided by GM Alternative Propulsion Center Europe, Germany, with contract number 4500456074NS2 titled "Impact and Crash Modeling of Thick Carbon Fiber-Reinforced Composite Structures Manufactured by Filament Winding".

References

1. Abrate, S., Impact on composite structures, Cambridge University Press, Cambridge, 1998
2. Hashin, Z, "Failure Criteria for Unidirectional Fiber Composites," *Journal of Applied Mechanics*, 1980, Vol. 47, pp. 329-334
3. Matzenmiller, A., Lubliner, J. and Taylor, R. L., "A constitutive model for anisotropic damage in fiber-composites," *Mechanics of Materials*, 1995, Vol. 20, No. 4, pp. 125–152
4. Gama, B. A., Haque, M. J., Gillespie Jr. J. W., Bogdanovich, A. E., "Impact, Damage, and Energy Absorption Of a 3D Orthogonal Weave Composite Unit Cell Model", *Proceedings of 49th International SAMPE Symposium and Exhibition*, Long Beach, CA, May 16–20, 2004
5. Xiao, J. R., Gama, B.A., and Gillespie Jr. J. W., "Progressive Damage Delamination in Plain Weave S-2 Glass/SC-15 Composites under Quasi-Static Punch-Shear Loading", *Composite Structures*, 2007, Vol. 78, pp. 182-196
6. Gama, B. A., Bogetti, T. A., and Gillespie Jr. J. W., "Composite Damage Modeling under Quasi-Static, Low Velocity Impact, Ballistic and Blast Loading Conditions", *SAMPE 2010*, Seattle, WA, May 17-20, 2010
7. LS-DYNA Keyword User's Manual, Livermore Software Technology Corporation. Version 971, May 2007
8. Belingardi, G., and Vadori, R., "Low Velocity Impact Tests of Laminate Glass-Fiber-Epoxy Matrix Composite Material Plates," *International Journal of Impact Engineering*, 2002, Vol. 27, pp. 213-229
9. Gama, B. A., Islam, S.M. W., Rahman, M., Gillespie Jr., J. W., Bogetti, T. A., Cheeseman, B. A., Yen, C-F., and Hoppel, C. P. R., "Punch Shear Behavior of Thick-Section Composites under Quasi-Static, Low Velocity, and Ballistic Impact Loading," *SAMPE Journal*, 2005, Vol. 41, No. 4, pp. 6-13